Received: 29 November 2023 | Revised: 9 January 2024 | Accepted: 18 January 2024 | Published online: 23 January 2024

RESEARCH ARTICLE

Journal of Optics and Photonics Research
2024, Vol. 1(1) 16–22
DOI: 10.47852/bonviewJOPR42022177

BON VIEW PUBLISHING

Modified Chalcogenide Glass Equations for the Activation Energy of Crystallization

Richard A. Loretz[1] and Thomas J. Loretz[2,*]

[1]*Nuclear Physics Consultant, USA*

[2]*Computer Engineering Service, USA*

Abstract: For over six decades, chalcogenide glasses (ChGs) have played a pivotal role in the optical community, fostering innovations and new applications in photonics, electronics, and electro-optics. In the last decade, the exploration of novel applications, such as Gradient Index (GRIN) ChGs, has underscored the need for a nuanced comprehension and precise control of nucleation and crystallization kinetics in emerging infrared glass compositions. This article explores the activation energy of crystallization in amorphous materials, particularly focusing on ChGs. It identifies long-standing challenges associated with existing models used for crystal growth in nucleated glasses. Employing carefully outlined mathematical logic, our study critiques conventional models and introduces innovative equations centering around the need for balanced units and proper physical trends. These new models overcome some shortcomings of the established framework and provide a more accurate depiction of crystallization kinetics. To validate the efficacy of our proposed models, we conducted a comparative analysis using differential scanning calorimetry data from a recently published Sb-Te-Se chalcogenide glass composition. The numerical and graphical results clearly illustrate the improvements inherent in our models and their practical utility. Beyond ChGs, our models and equations have broader applications. They may extend to oxide, halide, oxy-halide, and fluoride glass compositions, as well as polymers, contributing new tools to the understanding of crystallization kinetics across diverse materials.

Keywords: chalcogenide glass, activation energy of crystallization, GRIN glass, DSC analysis, crystal growth, infrared optics

1. Introduction

Differential scanning calorimetry (DSC) testing provides the quickest and most accurate means to determine the crystallization behavior of chalcogenide glasses (ChGs). These glasses contain neither oxygen nor any other anion. Unlike oxide glasses, they are not ionically bonded materials. Structurally, they are composed of van der Waals forces bonded and covalently bonded molecules, with the former being the more predominant percentage (Loretz et al., 2022). They are made by melting high atomic mass elements found in the periodic table and quenching the molecular melts to an amorphous state.

When DSC enthalpy data are collected and evaluated properly, optimum temperatures for nucleation and crystallization, as well as the correct activation energy for crystallization, can be determined readily. While the mathematics presented within this paper provides the foundations for the accurate solution of the optimum temperatures for nucleation and crystallization, we only address their use for determining the expression known as "the activation of crystallization." We will address the application of DSC endothermic and exothermic data to the task of determining the optimum (correct) temperatures for nucleation and crystallization in future publications.

Elabbar et al. (2008) published a chalcogenide glass research paper covering crystallization work done on a specific glass formula, found within the Sb-Te-Se compositional arena. They applied the traditional equations developed more than 80 years ago by Johnson, Mehl, and Avrami (the JMA model) (Avrami, 1939, 1940, 1941) in combination with those developed more than 55 years ago by Kissinger (1956) and Moynihan et al. (1974) to draw conclusions about the crystallization behavior of this amorphous material.

Starting with the JMA model, Equation (1), we derive new models and equations to replace those normally advocated in the literature but rarely given more than simple mathematical presentation and never given any mathematical justification, based on our literature review. These original models and equations are consistently applied to chalcogenide glass compositions during DSC studies (Abdel-Rahim et al., 2002; Augis & Bennett, 1978; Imran et al., 2001; Kissinger, 1957; Larmagnac et al., 1981; Lasocka, 1976; Matusita & Sakka, 1980; Moynihan et al., 1996; Ozawa, 1971; Patel & Pratap, 2012).

Our equations correct the irrational behavior, whereby key temperature points, such as the glass transition temperature (T_g), calculated using DSC enthalpy data collected from endothermic and/or exothermic results, migrate to absolute zero (along with the integrals over temperature) as DSC heating rates approach "0" degrees per unit time. Our new equations are temperature unit and time unit independent and allow for zero (i.e., final and true equilibrium) and near-zero heating rates to be evaluated without calculation errors (such as divide by zero). We provide a detailed mathematical explanation, which includes all logical steps.

*Corresponding author: Thomas J. Loretz, Computer Engineering Service, USA. Email: tom@CESWorldHQ.com

1.1. The original JMA equation

$$\frac{\alpha}{\alpha_\infty} = 1 - e^{-k\,t^n} \tag{1}$$

Where:
α is the volumetric fraction of crystallites at time t,
α_∞ is the maximum fractional volume of crystallites possible,
k is the reaction rate constant (reactions/unit time),
t is the reaction time, and
n is the "Avrami" exponent associated with nucleation and crystal growth mechanisms (unitless).

We cannot ignore the mathematically irrational nature of Equation (1), which raises "***e***" to a final power value that is neither unitless nor designed to have some type of useful fixed units, given that the time units contribution changes as ***n*** changes. Instead, we choose to accept the documented research of Khanna and Taylor (1988). Like us, they conclude that a mathematically rational model multiplies the reaction rate constant (***k***) with the reaction time (***t***) to create a unitless quantity which is then raised to the power of the Avrami constant, "***n***". They evaluated this model with material standards of known activation energy and confirmed their beliefs through controlled experiments.

1.2. The modified and corrected JMA equation

$$\frac{\alpha}{\alpha_\infty} = 1 - e^{-(k\,t)^n} \tag{2}$$

We will use this equation from this point forward and suggest that future researchers do the same, in light of its obvious mathematical correctness and more importantly, in light of its experimental validity. As explained above, this model does not suffer from the obvious mathematical imbalance of its predecessor.

1.3. The Arrhenius equation

Nucleation and crystallization are thermally activated processes and therefore as a salient element of the JMA process, the reaction rate constant *"**k**"* is related to the temperature by the Arrhenius equation:

$$k = A\ e^{-\frac{E}{RT}} \tag{3}$$

Where:
k is the reaction rate constant (1/unit time) for nucleation (k_N) or crystallization (k_C),
A is the pre-exponential factor (1/unit time) for nucleation (A_N) or crystallization (A_C),
E is the nucleation (E_n) or crystallization (E_c) activation energy (kJ mol^{-1}),
R is the gas constant (8.314e-03 kJ mol^{-1} °K^{-1}), and
T is the temperature (in °K) associated with nucleation (T_N) or crystallization (T_C).

For this paper, we are only interested in discussing the physics and mathematics of the crystallization process. Although we will not discuss the nucleation dynamics in this paper, the physics and mathematics of the process are expected to be similar. We will briefly discuss the misconceptions within our ChG community, which are associated with the determination of the correct nucleation and crystallization enthalpies for DSC analysis. However, we will ignore the effects of these issues for the purpose of this paper. The effects of these issues and corrections will be addressed in future papers by us and by our other team members.

The correct nucleation and crystallization enthalpies found within the boundaries of a DSC thermogram are those which would be located at the Limit "0" or, therefore, a heating rate of zero Kelvin degrees per unit time (alternately, zero degrees Celsius per unit time). Without exception, every ChG research paper we have studied ignores this requirement. Typically, the researchers elect to use a DSC sample heating rate of 10 °C/min or, worse yet, 20 °C/min, with no explanation or justification, leading us to conclude that researchers are simply doing what their colleagues are doing and not giving any consideration to why. Occasionally, we see measurements in the 3 to 5 °C/min range. However, these are rare and also without explanation. In future papers, we will explain why and how to use a DSC to measure at the Limit "0" to locate and evaluate all endotherms and exotherms.

Beyond the issue of location, the correctly chosen DSC crystallization enthalpy is a thermogram feature which starts at the baseline (zero enthalpy) and peaks at some positive value before declining in magnitude back to the baseline zero value (i.e., exothermic peak). Typically, the feature is symmetric in nature and its peak value provides the best temperature for controlled crystallization. Its internal area represents the sum of all heat flow (***dH/dt***) from t_0 to t_∞ [or the enthalpy at $t_\infty(\Delta H_\infty)$] and is readily integrated mathematically. Furthermore, the crystallization reaction rate constant (***k***) has a value of "0" at the start of the feature, experiences its largest value at the peak, and returns to zero at the end of the feature.

The problem with Equation (3) for a reaction rate approaching zero is that the temperature would need to approach absolute zero. Beyond the intuitive irrational nature of this issue, we know that this is not true, because the start of the crystallization process must occur at elevated temperatures that exceed the true glass transition temperature, T_g, for the amorphous material. This is to say that mechanically the glass may no longer exist within its elastic domain and must be in its inelastic domain, where relaxation time constants are quite small, allowing atoms to move freely throughout the amorphous matrix. For our reformulation of Equation (3), we are interested in seeing how reaction rate k varies with temperature relative to a given reaction rate k_1 at temperature T_1.

1.4. Our new mathematical model

$$\left(1 + \frac{k}{k_1}\right) = A' e^{\frac{-E_c}{R}\left[\frac{1}{T} - \frac{1}{T_1}\right]} \tag{4}$$

Where:
k is the reaction rate constant (reactions per unit time),
k_1 is the reaction rate constant linked with T_1,
A' is the pre-exponential factor (***unitless***),
E_C is activation energy "***density***" of crystallization (kJ mol^{-1}),
R is the gas constant (8.314e-03 kJ mol^{-1} °K^{-1}), and
T is the temperature (°K).

(Please refer to Appendix-A for mathematical proofs associated with the following derived equations presented)

1.5. Our modified Kissinger relationship

From Equation (4), k_i varies as $1/T_i$. The slope of $ln\left(\frac{\left(1+\frac{\beta_i}{\beta_1}\right)}{T_i^2}\right)$ vs $\left(\frac{1}{T_i}\right)$ is such that it follows our modified Kissinger relationship: $\frac{d\left(ln\left(\frac{\left(1+\frac{\beta_i}{\beta_1}\right)}{T_i^2}\right)\right)}{d\left(\left(\frac{1}{T_i}\right)\right)} = -\frac{E_C}{R}$,

where

$$\beta_1 = 1\ ^\circ K\ min^{-1} = \frac{1}{60}\ ^\circ K sec^{-1} = 60\ ^\circ K\ hr^{-1},\ \text{etc.} \qquad (19)$$

(Loretz & Loretz, 2024)

The units of the gas constant "**R**" are kJ mol^{-1} $^\circ K^{-1}$, and the term $\left[\frac{1}{T_i}\right]$ has units of $^\circ K^{-1}$. This makes $\frac{E_C}{R}\left[\frac{1}{T_i}\right]$ a unitless term. $\ln(T_i^2)$ has units $^\circ K^2$ and thus the term *Const* has units $^\circ K^{-2}$ {which is expected since it is proportional to $\ln\left[\left(\frac{1}{T_0}\right)^2\right]$}.

If we plot $\ln\left[\frac{\left(1+\frac{\beta_i}{\beta_1}\right)}{T_i^2}\right]$ vs $\left[\frac{1}{T_i}\right]$, the **slope** is $\left[-\frac{E_C}{R}\right]$ and will be different than that of the original formulation.

The value of the "***Activation Energy***" for any temperature domain of interest can be determined from our key equation:

$$[(-1)\ x\ R\ x\ (\textbf{slope})] = E_C \qquad (20)$$

(***Please refer to Appendix-B for mathematical proofs associated with the following derived equations presented***)

Using the derivation logic as detailed Appendix-B, Equation (B1b), the resulting ***MODIFIED*** model equation is

$$\left(1+\frac{\beta}{\beta_1}\right) = 2\left(\frac{T^2}{T_1^2}\right)e^{-\frac{E_C}{R}\left[\frac{1}{T}-\frac{1}{T_1}\right]} \qquad (30)$$

(***Please refer to Appendix-C for mathematical proofs associated with the following derived equations presented***)

A numerical comparison of the original and modified models [Equations (B5b) and (30), respectively] will be graphically demonstrated in the next section of the paper.

2. Experimentation

A DSC instrument provides a measurement of enthalpy (energy) per mol (differential power with time per unit mass of glass sample) as a function of a precision heating rate ($^\circ K\ sec^{-1}$). Power is defined as "work/time" (or, energy/time) and 1 Watt of power equals 1 J/sec. One mol is equal to 1.0 Avogadro's number of atoms of a material, where the mass of the glass sample equates to "***x***" mols of material (which is determined through knowledge of its density). Therefore, a calibrated and correctly applied DSC instrument provides graphical measurement values of differential energy per second per mol of glass ($\Delta J\ sec^{-1}\ mol^{-1}$), as a function of glass temperature increase per second ($\Delta^\circ K\ sec^{-1}$) for a given temperature ($^\circ K$), (or, $\Delta J\ mol^{-1}\ ^\circ K^{-1}$), a useful fact often overlooked. Table 1 is created using data extracted from the paper.

In accordance with our mathematical models, we make $\beta_1 = 1.0\ ^\circ K\ min^{-1}$. The data employed in our numerical example were taken from a recent research paper that examined the activation energy of a new composition of chalcogenide glass in the Se-Te-Sb family (or, by convention, Sb-Te-Selenide family).

The results of Table 1 are used to generate the two slope lines found in Figure 1. The red line represents the original slope determined by Elabbar, with its calculated activation energy of approximately 116.7 kJ per mol. The blue line represents our modified slope, with its corrected calculated activation energy of approximately 99.6 kJ per mol, which is significantly less (15%) energy to accomplish crystallization.

We believe that the change in activation energy is explained by the elimination of the inherent temperature approach to absolute zero of the original formulation and thus the use of a more physically rational temperature domain in the modified formulation.

Table 1
A comparison evaluation of the activation energy of crystallization for $Sb_{0.9}$-$Te_{20.0}$-$Se_{79.1}$ chalcogenide glass by applying traditional models and our models

T $^\circ K$	T^2 $^\circ K^2$	$\frac{1000}{T}$ $^\circ K^{-1}$	β/β_1 *Unitless*	$1+\frac{\beta}{\beta_1}$ *Unitless*	$\ln\left(\frac{\beta/\beta_1}{T^2}\right)$ $^\circ K^{-2}$	$ln\left(\frac{1+\frac{\beta}{\beta_1}}{T^2}\right)$ $^\circ K^{-2}$
400.0	160000	2.500	19.75	20.75	−9.00	−8.95
397.3	157846	2.517	15.95	16.95	−9.20	−9.14
396.2	156972	2.524	15.09	16.09	−9.25	−9.19
393.2	154635	2.543	13.45	14.45	−9.35	−9.28
390.5	152469	2.561	11.41	12.41	−9.50	−9.42
387.1	149883	2.583	8.31	9.31	−9.80	−9.69
384.0	147475	2.604	5.21	6.21	−10.25	−10.07
382.0	145902	2.618	4.02	5.02	−10.50	−10.28
379.5	144025	2.635	3.09	4.09	−10.75	−10.47
375.9	141331	2.660	1.93	2.93	−11.20	−10.78

Figure 1
Comparison of models for activation energy "slope" determination. The slope of the blue line is the accurate slope for use with Equation (19) to yield the activation energy of crystallization

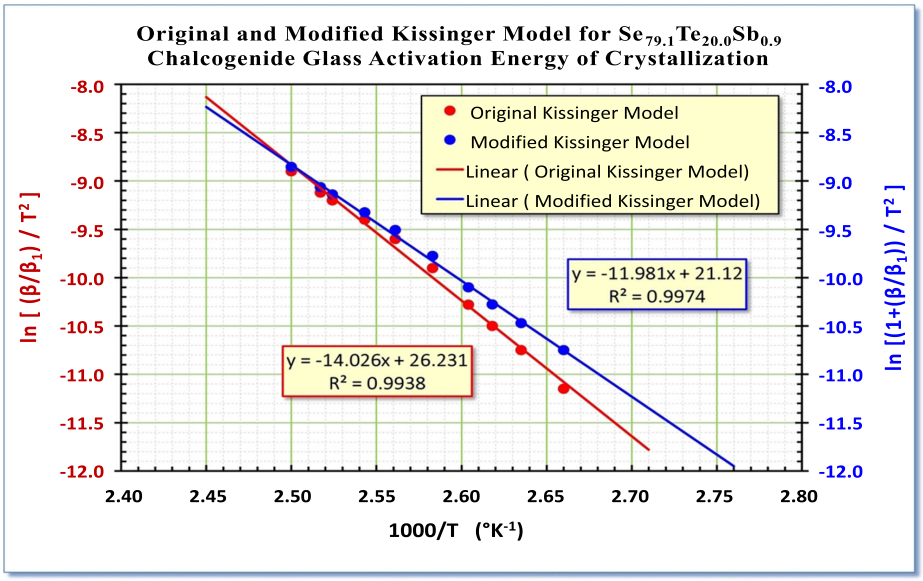

where per Equation (19): Modified Slope $= -11.98 = -E_c/R$, $E_c = -11.98 \times 8.315$ kJ mol^{-1} °K^{-1} $= 99.61$ kJ mol^{-1}.
Original Slope $= -14.03 = -E_c/R$, $E_c = -14.03 \times 8.315$ kJ mol^{-1} °K^{-1} $= 116.65$ kJ mol^{-1}.

3. Model Comparison

The original and modified models [Equations (B5b) and (30), respectively] can be evaluated numerically using the data from the above experiment. The result of the numerical calculations is shown visually in Figure 2. The original and modified curves follow the same trend with temperature, as expected, when higher heating rates are employed.

However, if one focuses on the low to near zero heating rate range, as depicted in Figure 3, it becomes obvious that the models diverge. This behavior is the consequence of the original formulation moving toward absolute zero temperatures as heating rates decrease, while

Figure 2
Comparison of heating rate versus temperature for the original and modified Kissinger formulations

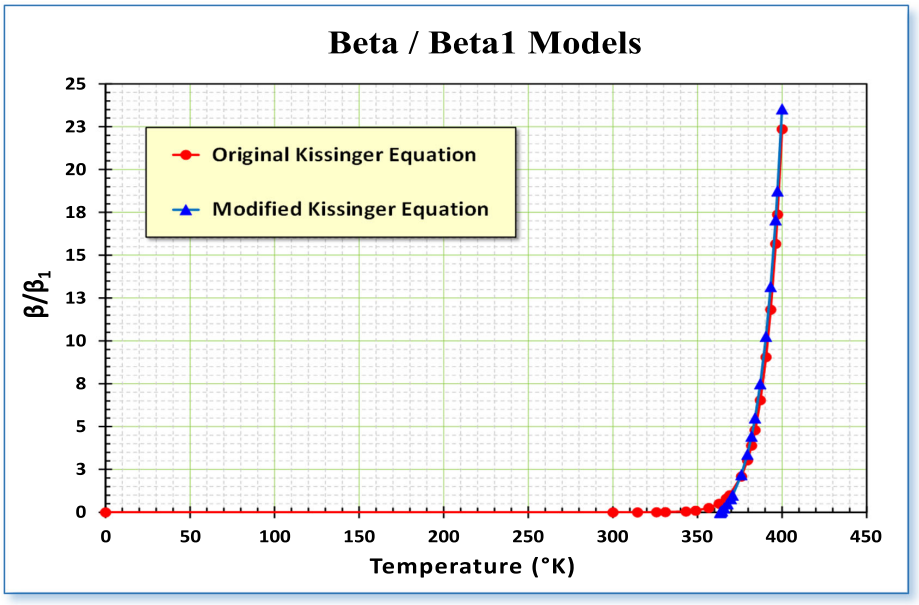

Figure 3
Reexamination of Figure 2 with focus on the low to near zero $\left(\frac{\beta}{\beta_1}\right)$ heating rate range

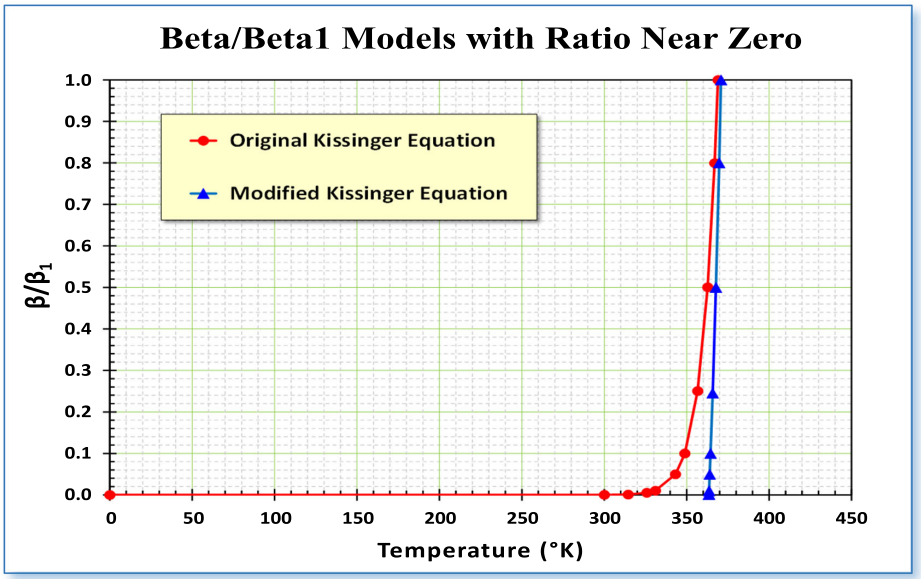

the modified model approaches a limiting temperature as heating rates decrease [a temperature which is slightly lower than T_1 (about 7 °K in this example, as shown below)].

From the numerical data, T_1 for the modified formulation is about 370.8 °K. This is the temperature where Equation (30) evaluates to $\frac{\beta}{\beta_1} = 1$. Using equation (C1) to solve for T_0 in terms of the value of T_1, the limiting temperature value is about $T_0 = 363.5$ °K, which is the intercept shown in Figure 3.

4. Conclusions and Discussion

For more than 55 years, chalcogenide glass (ChG) researchers have applied the Johnson–Mehl-Avrami (JMA) model in combination with either the Kissinger or Moynihan model to determine the activation energy for crystallization (Abd El-Raheem & Ali, 2010; Abu-Sehly et al., 2009; Afify, 1991; Ahmad et al., 2010; Al-Ghamdi et al., 2011; Aly, 2017; Dahshan et al., 2010; Kaur et al., 2000; Lee et al., 2004; Vázquez et al., 2004; Yinnon & Uhlmann, 1983). Individually and collectively, these models incorporate equations that have implicit shortcomings and which may lead to incorrect solutions, especially when employing slow heating rates. We have analyzed the equations associated with these models and corrected them to achieve necessary end results. We have provided the logical steps behind corrections and using DSC data found in published literature we have compared our solutions against those made with the original equations.

While we have only evaluated a modest number of research papers concerning ChG nucleation and crystallization, we have assessed a sufficient number of publications to feel confident that the reduction in energy demonstrated in this study will extend to other glass types as. We maintain this belief as a result of our work in the field of ChG science in general, where we have evaluated hundreds of peer reviewed papers covering DSC experimentation and analysis for a variety of other reasons. Unfortunately, most DSC data in the literature are taken at either 10 °C/min or 20 °C/min heating rates and therefore mispositions the true endothermic and exothermic enthalpies necessary for useful nucleation and crystallization data. For this reason, we expect that even larger and more profound variations will be generated in research studies which incorporate properly analyzed DSC nucleation and crystallization thermograms using data sets taken at the limit zero heating rate. We and our other team members will be providing further insight into this problem and its remedy in the near future.

The information provided in this paper offers a fundamental advancement in the field and a fresh perspective on the activation energy of crystallization in amorphous materials. By refining existing models and presenting new mathematical frameworks, it improves accuracy in describing nucleation and crystallization kinetics. This study should be particularly useful for researchers studying ChG Gradient Index (GRIN) compositions, where controlled variations in the refractive index are employed to focus light rather than traditional component geometry (Yadav et al., 2019). Typically, lasers and masks are used in combination with DSC nucleation and crystallization data to produce the desired lens performance. The application of these models to experimental data, particularly in the context of GRIN ChGs, underscores their importance and potential for widespread adoption in diverse material systems.

Recommendations

As researchers continue to develop highly specialized ChGs for optical, electro-optical, and electronic applications relying on nucleation and crystallization control, they will need access to more accurate activation energy information than presently available using current mathematical models. They will also need access to accurate information concerning nucleation and crystallization temperatures. Without such data, a useful process can neither be developed nor optimized. We believe that such accuracies can only be achieved by analyzing endothermic and exothermic behaviors properly and then applying the models and equations provided by us in this paper. Lastly, we believe that our

models can be used in most other material fields (such as polymers) where DSC is employed to generate similar enthalpy data.

Acknowledgment

Co-author Thomas Loretz recognized the need for this paper after many years of mutual collaboration with Dr. Kathleen A. Richardson, her students and colleagues at the University of Central Florida, CREOL division. Dr. Richardson is one of the world's leading authorities on chalcogenide glass science and has provided helpful comments and encouragement throughout our journey.

Ethical Statement

This study does not contain any studies with human or animal subjects performed by any of the authors.

Conflicts of Interest

The authors declare that they have no conflicts of interest to this work.

Data Availability Statement

Data sharing not applicable—no new data generated. All data used in calculations were extracted from Elabbar et al. (2008).

References

Abd El-Raheem, M. M., & Ali, H. M. (2010). Crystallization kinetics determination of $Pb_{15}Ge_{27}Se_{58}$ chalcogenide glass by using the various heating rates (VHR) method. *Journal of Non-Crystalline Solids*, *356*(2), 77–82. https://doi.org/10.1016/j.jnoncrysol.2009.10.010

Abdel-Rahim, M. A., Abdel-Latief, A. Y., Soltan, A. S., & El-Oyoun, M. A. (2002). Crystallization kinetics of overlapping phases in $Cu_6Ge_{14}Te_{80}$ chalcogenide glass. *Physica B: Condensed Matter*, *322*(3–4), 252–261. https://doi.org/10.1016/S0921-4526(02)01190-0

Abu-Sehly, A. A., Alamri, S. N., & Joraid, A. A. (2009). Measurements of DSC isothermal crystallization kinetics in amorphous selenium bulk samples. *Journal of Alloys and Compounds*, *476*(1–2), 348–351. https://doi.org/10.1016/j.jallcom.2008.08.059

Afify, N. (1991). Kinetics study of non-isothermal crystallization in $Se_{0.7}Te_{0.3}$ chalcogenide glass. *Journal of Non-Crystalline Solids*, *136*(1–2), 67–75. https://doi.org/10.1016/0022-3093(91)90120-U

Ahmad, A., Khan, S. A., Al-Ghamdi, A. A., Al-Agel, F. A., Sinha, K., Zulfequar, M., & Husain, M. (2010). Kinetics of non-isothermal crystallization of ternary $Se_{80}Te_{20-x}Zn_x$ glasses. *Journal of Alloys and Compounds*, *497*(1–2), 215–220. https://doi.org/10.1016/j.jallcom.2010.03.015

Al-Ghamdi, A. A., Alvi, M. A., & Khan, S. A. (2011). Non-isothermal crystallization kinetic study on $Ga_{15}Se_{85-x}Ag_x$ chalcogenide glasses by using differential scanning calorimetry. *Journal of Alloys and Compounds*, *509*(5), 2087–2093. https://doi.org/10.1016/j.jallcom.2010.10.145

Aly, K. A. (2017). Crystallization study of Se_{86} Sb_{14} glass: A new method to determine the kinetic exponent (n) with high accuracy. *Journal of Thermal Analysis and Calorimetry*, *129*(2), 709–714. https://doi.org/10.1007/s10973-017-6283-7

Augis, J. A., & Bennett, J. E. (1978). Calculation of the Avrami parameters for heterogeneous solid state reactions using a modification of the Kissinger method. *Journal of Thermal Analysis*, *13*(2), 283–292. https://doi.org/10.1007/BF01912301

Avrami, M. (1939). Kinetics of phase change. I general theory. *The Journal of Chemical Physics*, *7*(12), 1103–1112. https://doi.org/10.1063/1.1750380

Avrami, M. (1940). Kinetics of phase change. II transformation-time relations for random distribution of nuclei. *The Journal of Chemical Physics*, *8*(2), 212–224. https://doi.org/10.1063/1.1750631

Avrami, M. (1941). Granulation, phase change, and microstructure kinetics of phase change. III. *The Journal of Chemical Physics*, *9*(2), 177–184. https://doi.org/10.1063/1.1750872

Dahshan, A., Amer, H. H., & Aly, K. A. (2010). Thermal stability and crystallization kinetics of Ge–Se–Cd glasses. *Philosophical Magazine*, *90*(11), 1435–1449. https://doi.org/10.1080/14786430903397271

Elabbar, A. A., El-Oyoun, M. A., & Abu-Sehly, A. A. (2008). Evaluation of the activation energy of crystallization in $Se_{79.1}Te_{20}Sb_{0.9}$ chalcogenide glass using isoconversional methods. *Journal of Taibah University for Science*, *1*, 44–50.

Imran, M. M. A., Bhandari, D., & Saxena, N. S. (2001). Kinetic studies of bulk $Ge_{22}Se_{78-x}Bi_x$ (x=0, 4 and 8) semiconducting glasses. *Journal of Thermal Analysis and Calorimetry*, *65*(1), 257–274. https://doi.org/10.1023/a:1011557425244

Kaur, G., Komatsu, T., & Thangaraj, R. (2000). Crystallization kinetics of bulk amorphous Se-Te-Sn system. *Journal of Materials Science*, *35*(4), 903–906. https://doi.org/10.1023/A:1004798308059

Khanna, Y. P., & Taylor, T. J. (1988). Comments and recommendations on the use of the Avrami equation for physico-chemical kinetics. *Polymer Engineering and Science*, *28*(16), 1042–1045. https://doi.org/10.1002/pen.760281605

Kissinger, H. E. (1956). Variation of peak temperature with heating rate in differential thermal analysis. *Journal of Research of the National Bureau of Standards*, *57*(4), 217–221. https://doi.org/10.6028/jres.057.026

Kissinger, H. E. (1957). Reaction kinetics in differential thermal analysis. *Analytical Chemistry*, *29*(11), 1702–1706. https://doi.org/10.1021/ac60131a045

Larmagnac, J. P., Grenet, J., & Michon, P. (1981). Glass transition temperature dependence on heating rate and on ageing for amorphous selenium films. *Journal of Non-Crystalline Solids*, *45*(2), 157–168. https://doi.org/10.1016/0022-3093(81)90184-8

Lasocka, M. (1976). The effect of scanning rate on glass transition temperature of splat-cooled $Te_{85}Ge_{15}$. *Materials Science and Engineering*, *23*(2–3), 173–177. https://doi.org/10.1016/0025-5416(76)90189-0

Lee, C. M., Lin, Y. I., & Chin, T. S. (2004). Crystallization kinetics of amorphous Ga–Sb–Te chalcogenide films: Part I. Nonisothermal studies by differential scanning calorimetry. *Journal of Materials Research*, *19*(10), 2929–2937. https://doi.org/10.1557/JMR.2004.0378

Loretz, R. A., Loretz, T. J., & Richardson, K. A. (2022). Predictive method to assess chalcogenide glass properties: Bonding, density and the impact on glass properties. *Optical Materials Express*, *12*(5), 2012–2027. https://doi.org/10.1364/OME.455523

Loretz, R. A., & Loretz, T. J. (2024). Corrections to theoretical glass transition temperature models and interpretations with application examples to chalcogenide glass. *Journal of Non-Crystalline Solids*, *628*, 122845. https://doi.org/10.1016/j.jnoncrysol.2024.122845

Matusita, K., & Sakka, S. (1980). Kinetic study of crystallization of glass by differential thermal analysis—Criterion on application of Kissinger plot. *Journal of Non-Crystalline Solids*, *38–39*, 741–746. https://doi.org/10.1016/0022-3093(80)90525-6

Moynihan, C. T., Easteal, A. J., Wilder, J., & Tucker, J. (1974). Dependence of the glass transition temperature on heating and cooling rate. *The Journal of Physical Chemistry*, *78*(26), 2673–2677. https://doi.org/10.1021/j100619a008

Moynihan, C. T., Lee, S. K., Tatsumisago, M., & Minami, T. (1996). Estimation of activation energies for structural relaxation and viscous flow from DTA and DSC experiments. *Thermochimica Acta*, *280–281*, 153–162. https://doi.org/10.1016/0040-6031(95)02781-5

Ozawa, T. (1971). Kinetics of non-isothermal crystallization. *Polymer*, *12*(3), 150–158. https://doi.org/10.1016/0032-3861(71)90041-3

Patel, A. T., & Pratap, A. (2012). Study of kinetics of glass transition of metallic glasses. *Journal of Thermal Analysis and Calorimetry*, *110*(2), 567–571. https://doi.org/10.1007/s10973-012-2527-8

Vázquez, J., Barreda, D. G. G., López-Alemany, P. L., Villares, P., & Jiménez-Garay, R. (2004). Crystallization of $Ge_{0.08}Sb_{0.15}Se_{0.77}$ glass studied by DSC. *Journal of Non-Crystalline Solids*, *345–346*, 142–147. https://doi.org/10.1016/j.jnoncrysol.2004.08.012

Yadav, A., Buff, A., Kang, M., Sisken, L., Smith, C., Lonergan, J., . . . , & Richardson, K. A. (2019). Melt property variation in $GeSe_2$-As_2Se_3-PbSe glass ceramics for infrared gradient refractive index (GRIN) applications. *International Journal of Applied Glass Science*, *10*(1), 27–40. https://doi.org/10.1111/ijag.12618

Yinnon, H., & Uhlmann, D. R. (1983). Applications of thermoanalytical techniques to the study of crystallization kinetics in glass-forming liquids, part I: Theory. *Journal of Non-Crystalline Solids*, *54*(3), 253–275. https://doi.org/10.1016/0022-3093(83)90069-8

How to Cite: Loretz, R. A., & Loretz, T. J. (2024). Modified Chalcogenide Glass Equations for the Activation Energy of Crystallization. *Journal of Optics and Photonics Research*. *1*(1), 16–22. https://doi.org/10.47852/bonviewJOPR42022177

Appendices

Appendix-A

We can solve for $\mathbf{A}'$ when $\boldsymbol{k}$ equals $\boldsymbol{k_1}$ at temperature T equals T_1:

$$\left(1+\frac{k_1}{k_1}\right) = A' e^{-\frac{E_c}{R}\left[\frac{1}{T_1}-\frac{1}{T_1}\right]} \tag{A1a}$$

$$2 = A'\, e^{-\frac{E_c}{R}[0]} = A' \tag{A1b}$$

In the limit as k approaches "zero" and T approaches T_0, and Equation (4) becomes:

$$1+0 = 2e^{-\frac{E_c}{R}\left[\frac{1}{T_0}-\frac{1}{T_1}\right]} \tag{A2a}$$

$$\frac{1}{2} = e^{-\frac{E_c}{R}\left[\frac{1}{T_0}-\frac{1}{T_1}\right]} \tag{A2b}$$

$$-\frac{E_c}{R}\left[\frac{1}{T_0}-\frac{1}{T_1}\right] = ln\left(\frac{1}{2}\right) \tag{A2c}$$

$$T_0 = \left[\frac{1}{T_1}+\frac{R}{E_c}ln(2)\right]^{-1} \tag{A2d}$$

Thus, we can express Equation (4) in terms of the limiting temperature T_0 as

$$\left(1+\frac{k}{k_1}\right) = 2e^{-\frac{E_c}{R}\left[\frac{1}{T}+\frac{R}{E_C}ln(2)-\frac{1}{T_0}\right]} \quad \text{or} \tag{A3a}$$

$$ln\left(1+\frac{k}{k_1}\right) = ln(2) - \frac{E_C}{R}\left[\frac{1}{T}-\frac{1}{T_0}\right] - ln(2) \tag{A3b}$$

$$ln\left(1+\frac{k}{k_1}\right) = -\frac{E_C}{R}\left[\frac{1}{T}-\frac{1}{T_0}\right] \tag{A3c}$$

The derivative of Equation (A3c) with respect to time is

$$\frac{d}{dt}ln\left(1+\frac{k}{k_1}\right) = \frac{d}{dt}\left[-\frac{E_C}{R}\left[\frac{1}{T}-\frac{1}{T_0}\right]\right] \tag{A4a}$$

$$\frac{1/k_1}{\left(1+\frac{k}{k_1}\right)}\frac{dk}{dt} = \frac{E_C}{R}\,T^{-2}\,\frac{dT}{dt} \tag{A4b}$$

$$\frac{dk}{dt} = (k_1+k)\frac{E_C}{R}\,T^{-2}\,\frac{dT}{dt} \text{ or} \tag{A4c}$$

$$\frac{dk}{dt} = k_1\left(1+\frac{k}{k_1}\right)\frac{E_C}{R}\,T^{-2}\,\frac{dT}{dt} \tag{A4d}$$

Returning to Equation (2), the derivative of the fractional crystalline volume with respect to time is

$$\frac{1}{\alpha_\infty}\frac{d\alpha}{dt} = \left[-n(kt)^{n-1}\left[t\,\frac{dk}{dt}+k\,\frac{dt}{dt}\right]\right]e^{-(kt)^n} \tag{A5a}$$

$$\frac{1}{\alpha_\infty}\frac{d\alpha}{dt} = \left[-n(kt)^{n-1}\left[t\,\frac{dk}{dt}+k\right]\right]e^{-(kt)^n} \tag{A5b}$$

Substituting Equation (A4d) yields:

$$\frac{1}{\alpha_\infty}\frac{d\alpha}{dt} = \left[-n(kt)^{n-1}\left[k_1 t\left(1+\frac{k}{k_1}\right)\frac{E_C}{R}\,T^{-2}\,\frac{dT}{dt}+k\right]\right]e^{-(kt)^n} \tag{A6}$$

If the heating rate is constant such that $\frac{dT}{dt} = \beta$, then Equation (A6) becomes:

$$\frac{1}{\alpha_\infty}\frac{d\alpha}{dt} = \left[-n(kt)^{n-1}\left[k_1 t\left(1+\frac{k}{k_1}\right)\frac{E_C}{R}\,T^{-2}\,\beta+k\right]\right]e^{-(kt)^n} \tag{A7}$$

Now, when $k = k_i$, the Equation (A7) for $\frac{d\alpha_i}{dt}$ becomes:

$$\frac{1}{\alpha_\infty}\frac{d\alpha_i}{dt} = \left[-n(k_i t)^{n-1}\left[k_1 t\left(1+\frac{k_i}{k_1}\right)\frac{E_C}{R}\,T_i^{-2}\,\beta_i+k_i\right]\right]e^{-(k_i t)^n} \tag{A8}$$

Taking the natural log of both sides yields:

$$ln\left(\frac{1}{\alpha_\infty}\frac{d\alpha_i}{dt}\right) = ln\left[-n(k_i t)^{n-1}k_1 t\left(1+\frac{k_i}{k_1}\right)\frac{E_C}{R}T_i^{-2}\,\beta_i - n(k_i t)^{n-1}k_i\right] - (k_i t)^n \text{ or} \tag{A9a}$$

$$ln\left(\frac{1}{\alpha_\infty}\frac{d\alpha_i}{dt}\right) = ln\left[-nk_1(k_i)^{n-1}t^n\left(1+\frac{k_i}{k_1}\right)\frac{E_C}{R}T_i^{-2}\,\beta_i - n(k_i)^n(t)^{n-1}\right] - (k_i t)^n \tag{A9b}$$

When $k_i = k_1$, $T_i = T_1$, $\beta_i = \beta_1$ and $\alpha_i = \alpha_1$, then Equation (A9b) yields:

$$ln\left(\frac{1}{\alpha_\infty}\frac{d\alpha_1}{dt}\right) = ln\left[-nk_1(k_1)^{n-1}t^n\left(1+\frac{k_1}{k_1}\right)\frac{E_C}{R}T_1^{-2}\,\beta_1 - n(k_1)^n(t)^{n-1}\right] - (k_1 t)^n \tag{A10}$$

Rearranging terms yields:

$$ln\left(\frac{1}{\alpha_\infty}\frac{d\alpha_1}{dt}\right) = ln\left[-n(k_1)^n\,t^n\left[(2)\,\frac{E_C}{R}\,T_1^{-2}\,\beta_1 + (t)^{-1}\right]\right] - (k_1 t)^n \tag{A11}$$

Thus,

$$\frac{1}{\alpha_\infty}\frac{d\alpha_1}{dt} = -n(k_1)^n\,t^n\left[(2)\,\frac{E_C}{R}\,T_1^{-2}\,\beta_1 + (t)^{-1}\right]e^{-(k_1 t)^n} \tag{A12}$$

Integrating Equation (A12) vs fractional volume yields:

$$\int_0^{\alpha_\infty}\frac{1}{\alpha_\infty}d\alpha_1 = \int_0^{t_{final}} -n\,(k_1 t)^{n-1}k_1\left[(2)\,\frac{E_C}{R}\,\frac{\beta_1}{T_1^2}t + 1\right]e^{-(k_1 t)^n}dt \tag{A13}$$

The left-hand side (LHS) of Equation (A13) integrates to unity. This has to equal the integral of the right-hand side (RHS) of the equation

as the "final time" (t_{final}) approaches infinity. The right-hand side of Equation (A13) can be rewritten as

$$\lim_{tfinal\to\infty}\int_0^{t_{final}} -n\,(k_1t)^{n-1}k_1\left[(2)\,\frac{E_C}{R}\,\frac{\beta_1}{T_1^2}t+\,1\right]e^{-(k_1t)^n}dt = \lim_{tfinal\to\infty}\int_0^{t_{final}} -n\,(k_1t)^{n-1}\,k_1\,(2)\frac{E_C}{R}\,\frac{\beta_1}{T_1^2}\,t\,e^{-(k_1t)^n}dt + \lim_{tfinal\to\infty}\int_0^{t_{final}} -n\,(k_1t)^{n-1}k_1e^{-(k_1t)^n}dt \tag{A14}$$

The first term on the RHS of Equation (A14) is the fractional volume contribution from a varying reaction rate versus time (***varying temperature induced***). The second term on the RHS of Equation (A14) is the fractional volume contribution from the fixed portion of the reaction rate. Thus, ***if dT/dt equals 0***, meaning that the reaction rate, k_1, stays constant (***and the temperature stays constant***), the first RHS integral also equals zero and the second RHS integral will eventually get to unity ("**1**") as time approaches infinity, assuming one is at a favorable temperature for crystallization to occur.

However, ***when dT/dt is greater than zero***, the first term of the RHS of Equation (A14) is nonzero, implying that both terms may contribute toward a unity solution (and the solution may reach "saturation" in less time). On the contrary, however, an ever-increasing temperature due to heating, especially if the heating rate is high, may reduce the time spent in the favorable crystallization temperature range, thus reducing the amount of crystallization that can occur. Thus, constant temperature or slow heating rates may accomplish more complete crystallization than fast heating rates. The fractional volume of crystals in the glassy matrix will try to approach α_∞ providing the material remains in favorable temperatures for crystallization. The physical implication of the fractional volume achieving α_∞ is that no further reactions can take place, as a consequence of all available nucleation sites either being consumed or being separated by a kinetically prohibitive distance that prevents further crystallization.

Appendix-B

We turn our attention to the issue of units, an issue frequently ignored by the glass community. The RHS of Equation (B1) has to match the units of the LHS. $\frac{E_C}{R}$ has units of °K. Thus, the LHS must also have the units °K.

$$\text{Let}\,x_i = \left(\frac{1}{T_i}\right)\text{Then,}\;\frac{d(ln((1+\beta_i/\beta_1)x_i^2)}{d\,((x_i))} = \left[\left(1+\frac{\beta_i}{\beta_1}\right)X^2\right]^{-1}\left(\frac{d\beta/dX}{\beta_1}\,X^2+\,\left(1+\frac{\beta}{\beta_1}\right)2\,X\right) \tag{B1a}$$

$$\frac{d(\ln((1+\beta_i/\beta_1)x_i^2)}{d\,((x_i))} = \frac{1}{(\beta_1+\,\beta)}\,\frac{d\beta}{dX}+\frac{2}{X} = -\,\frac{E_C}{R} \tag{B1b}$$

Substituting $\frac{1}{T_i}$ for x_i yields:

$$\frac{d(ln((1+\beta_i/\beta_1)T_i^{-2})}{d\,((T_i^{-1}))} = \frac{1}{(\beta_1+\,\beta)}\,\frac{d\beta}{d\,((T_i^{-1}))}+\,2T \tag{B2}$$

and the units of both terms of the RHS of Equation (B2) are thus °K, as expected.

Researchers have expressed an equation which is similar to our Equation (B1) (Moynihan et al., 1974):

$$\frac{d\left(ln\left(\frac{\beta_i}{T_i^2}\right)\right)}{d\left(\left(\frac{1}{T_i}\right)\right)} = -\,\frac{E_C}{R} \tag{B3}$$

These researchers either do not recognize or perhaps choose not to acknowledge that this equation's LHS has time units (ex. 1/min) in the β_i term. The equation, as written, will be numerically challenged when β_i changes units from °K/min to °K/sec to °K/hr. For instance, not only do the numeric values change with unit changes but also there can be a sign change when a particular value of $\frac{\beta_i}{T_i^2}$ goes from less than unity to greater than unity (i.e., the natural log of a number less than unity is negative and the natural log of a number greater or equal to unity is positive). Equation (B3) can be corrected for time units by expressing it as

$$\frac{d\left(ln\left(\frac{\beta_i/\beta_1}{T_i^2}\right)\right)}{d\left(\left(\frac{1}{T_i}\right)\right)} = -\,\frac{E_C}{R} \tag{B4}$$

where $\beta_1 = 1\,^\circ K\,min^{-1} = \frac{1}{60}\,^\circ Ksec^{-1} = 60\,^\circ K\,hr^{-1},\ etc.$

Although Equation (B4) has addressed the potential unit issues, there is another, more important, problem with the original formulation that is revealed below.

$$Let\;x_i = \left(\frac{1}{T_i}\right).$$

Then Equation (B4) becomes

$$\frac{d\;\ln[(\beta\,/\beta_1)X^2]}{d\,[X]} = -\frac{E_C}{R} = [\beta/\beta_1\,X^2]^{-1}\left[X^2\left(\frac{1}{\beta_1}\right)\frac{d\beta}{dX}+2\left(\frac{\beta}{\beta_1}\right)X\right] \tag{B5a}$$

$$\text{or}\qquad \frac{d\;\ln[(\beta\,/\beta_1)X^2]}{d\,[X]} = \left[\frac{1}{\beta}\,\frac{d\beta}{dX}+\frac{2}{X}\right] = -\,\frac{E_C}{R} \tag{B5b}$$

Rearranging Equation (B5b) and integrating yields:

$$\int_{\beta_1}^{\beta}\frac{1}{\beta}\,d\beta = \ln(\beta)-\ln(\beta_1) = \int_{X_1}^{X}\left[-\frac{E_C}{R}-\,\frac{2}{X}\right]dX = -\frac{E_C}{R}\,[X-\,X_1]-2\ln(X)+2\,\mathbf{ln}(X_1) \tag{B6}$$

or, after substituting $\left(\frac{1}{T_i}\right) = x_i$ and evaluating terms results in:

$$\ln\left(\frac{\beta}{\beta_1}\right) = -\frac{E_C}{R}\left[\frac{1}{T} - \frac{1}{T_1}\right] + \ln\left(\frac{T^2}{T_1^2}\right) \tag{B7}$$

Taking the inverse natural log of both sides of Equation (B7) yields the ***ORIGINAL*** model equation is

$$\left(\frac{\beta}{\beta_1}\right) = \left(\frac{T^2}{T_1^2}\right) e^{-\frac{E_C}{R}\left[\frac{1}{T} - \frac{1}{T_1}\right]} \tag{B8}$$

If one evaluates Equation (B8) in the limit of zero heating rate, one obtains the following relationship to the limiting zero heating temperature T_0:

$$\lim_{\beta \to 0}\left(\frac{\beta}{\beta_1}\right) = \left(\frac{{T_0}^2}{T_1^2}\right) e^{-\frac{E_C}{R}\left[\frac{1}{T_0} - \frac{1}{T_1}\right]} = 0 \tag{B9}$$

The only way to satisfy Equation (B9) is for the temperature T_0 to approach absolute zero. The reality is that we do not see such a plunge in temperature if, for instance, very low heating rates are utilized in a DSC or the DSC is turned off all together. Luckily, a more precise physical model can be developed using the relationship of Equation (B1b).

Appendix-C

For the relationship of a **zero-valued heating rate to temperature** T_0, the resulting equation is

$$\lim_{\beta \to 0}\left(\frac{\beta}{\beta_1}\right) = \left[2\left(\frac{T_0^2}{T_1^2}\right) e^{-\frac{E_C}{R}\left[\frac{1}{T_0} - \frac{1}{T_1}\right]}\right] - 1 = 0 \tag{C1}$$

Equation (C1) shows that there is a temperature T_0 associated with a zero-valued heating rate that is not tied to absolute zero. In fact, the temperature T_0 is related to temperature T_1 by

$$2\,ln(T_0) - \frac{E_C}{R}\left[\frac{1}{T_0}\right] = -\ln(2) + 2\ln(T_1) - \frac{E_C}{R}\left[\frac{1}{T_1}\right] \tag{C2}$$